OPEN ACCESS

Phase estimation from atom position measurements

New Journal of Physics
The open-access journal for physics

Phase estimation from atom position measurements

J Chwedeńczuk[1,3], F Piazza[2] and A Smerzi[2]

[1] Faculty of Physics, University of Warsaw, Poland
[2] INO-CNR, BEC Center, Via Sommarive 14, 38123 Povo, Trento, Italy
E-mail: jan.chwedenczuk@fuw.edu.pl

New Journal of Physics **13** (2011) 065023 (18pp)
Received 16 December 2010
Published 28 June 2011
Online at http://www.njp.org/
doi:10.1088/1367-2630/13/6/065023

Abstract. We study the measurement of the positions of atoms as a means of estimating the relative phase between two Bose–Einstein condensates. We consider N bosonic atoms released from a double-well trap, which form an interference pattern; we show that the measurement of the position of N atoms has a sensitivity that saturates the bound set by the quantum Fisher information, and allows for estimation at the Heisenberg limit of precision. Phase estimation through the measurement of the center of mass of the interference pattern can also provide sub-shot-noise sensitivity. Finally, we study the effect of an overlap of the two clouds on the estimation precision when Mach–Zehnder interferometry is performed in a double well. We find that a nonzero overlap of the clouds strongly reduces the phase sensitivity.

[3] Author to whom any correspondence should be addressed.

Contents

1. Introduction

Interferometry aims to estimate the relative phase between two wave packets. In the standard optical interferometer, such as the well-known Mach–Zehnder setup [1], the two wave packets correspond to the light traveling inside the two arms of the device, and the relative phase θ is acquired, for instance, as a result of different optical path lengths. After the phase is accumulated, the two wave packets are recombined through a beam splitter, and the signal at the two output ports depends on θ. The phase can be estimated by measuring the difference in intensity between these ports. Apart from photons, atoms can also be employed for interferometric purposes [2]. Atoms have some interesting advantages over light, especially due to the nonzero mass. In particular, the creation of atomic Bose–Einstein condensates (BECs) opened a new chapter in the field of interferometry. The BEC, which behaves like a macroscopic matter-wave, constitutes a coherent and controllable source of particles. This makes the BEC a promising system to measure electromagnetic [3–5] or gravitational [6–8] forces. Moreover, the inter-atomic interactions in the BEC are a source of nonlinearity, which can be used to create nonclassical states [9–12] that are useful in overcoming the limit imposed by classical physics on measurement precision [13, 14].

A BEC interferometer can be implemented using a double-well trap [15–24], where the two wave packets are localized about the two minima of the external potential. In such a configuration, a relative phase θ can be accumulated by letting the system evolve in time in the presence of an energy difference between the two potential minima, and in the absence of coupling between the two wells. After this stage, one can, for example, recombine the wave packets by implementing a beam splitter (thereby realizing a Mach–Zehnder interferometer (MZI)). This will imply a further dynamical evolution during which atoms oscillate between the wells for a time that must be precisely under control, and over which interactions are negligible.

In this paper, we study the sensitivity and double-well implementation of a new interferometer, simpler than the Mach–Zehnder, which consists of just a phase shifter performed in-trap, followed by a free expansion of the atomic cloud. By releasing the atoms from the double-well trap, the wave packets expand and overlap, thereby forming an interference pattern, as shown in figure 1. We discuss how the information about the phase can be extracted from this pattern and derive the sensitivity for different estimation strategies. Apart from the technological relevance deriving from a simpler implementation, the interferometer studied here is also conceptually interesting, since the interference pattern contains a great deal of fundamental information about the nature of the quantum many-body state and has been widely studied since the realization of atomic BECs.

The paper is organized as follows. In section 2, we formulate the problem and introduce the formalism. In section 3, we show that when estimation is performed using the positions of all of the atoms in the cloud, the sensitivity saturates the bound set by the quantum Fisher information (QFI) [25] and can reach the Heisenberg limit. Then, in section 4, we analyze an estimation scheme based on the detection of the position of the center of mass of the interference pattern, which can still yield sub-shot-noise sensitivity. Finally, in section 5, we study the sensitivity of the MZI, and we note that a nonzero overlap between the wave packets significantly reduces the sensitivity. Details of the calculations are presented in the appendix. The present paper is an extension of our previous work [26].

2. The model

In the following discussion of different estimation methods based on the measurement of the positions of the atoms, we will employ the two-mode approximation for a bosonic gas in a double-well potential, corresponding to the field operator

$$\hat{\Psi}(x,t) = \psi_a(x,t)\hat{a} + \psi_b(x,t)\hat{b},$$

where $\hat{a}^\dagger/\hat{b}^\dagger$ creates an atom in the left/right well.

In the interferometric sequence that we want to study, the first stage consists of a phase shifter, taking place with the atoms still trapped in the double well, by which a relative phase θ is imprinted between the modes. If the time scale is such that both the hopping between the wells and the atom–atom interactions are negligible, this stage is simply represented by the unitary evolution

$$\hat{U}(\theta) = \mathrm{e}^{-\mathrm{i}\theta\hat{J}_z} \tag{1}$$

of the initial state $|\psi_{\mathrm{in}}\rangle$ of the double-well system. The three operators

$$\hat{J}_x \equiv (\hat{a}^\dagger\hat{b} + \hat{b}^\dagger\hat{a})/2, \quad \hat{J}_y \equiv (\hat{a}^\dagger\hat{b} - \hat{b}^\dagger\hat{a})/2i \quad \text{and} \quad \hat{J}_z \equiv (\hat{a}^\dagger\hat{a} - \hat{b}^\dagger\hat{b})/2$$

form a closed algebra of angular momentum. In the next, and final, interferometric stage, the double-well trap is switched off, and the two clouds described by the mode functions $\psi_{a/b}(x,t)$ freely expand.

The most general quantity, containing statistical information about the positions of the particles forming the interference pattern [27–29], is the conditional probability of finding N particles at positions $\vec{x}_N = (x_1 \cdots x_N)$. This can be expressed in terms of the Nth-order correlation function $p_N(\vec{x}_N|\theta) = \frac{1}{N!}G_N(\vec{x}_N,\theta)$, where

$$G_N(\vec{x}_N,\theta) = \langle\psi_{\mathrm{out}}|\hat{\Psi}^\dagger(x_1,t)\cdots\hat{\Psi}^\dagger(x_N,t)\hat{\Psi}(x_N,t)\cdots\hat{\Psi}(x_1,t)|\psi_{\mathrm{out}}\rangle.$$

Here, $|\psi_{\mathrm{out}}\rangle$ denotes the state after the phase shift transformation, $|\psi_{\mathrm{out}}\rangle = \mathrm{e}^{-\mathrm{i}\theta\hat{J}_z}|\psi_{\mathrm{in}}\rangle$.

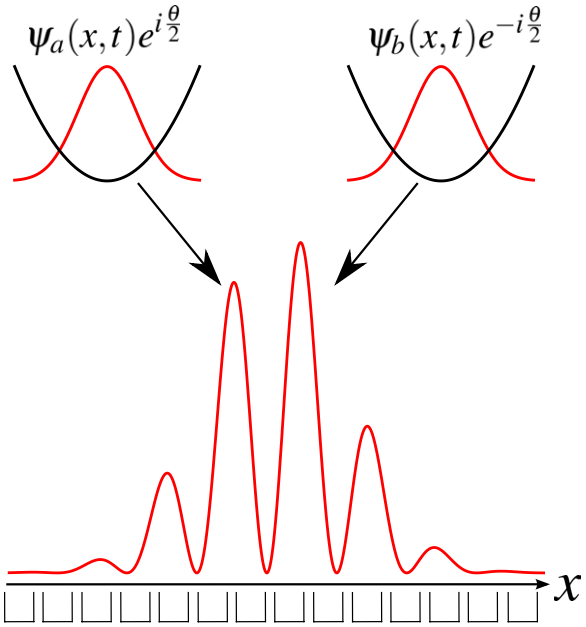

Figure 1. Schematic representation of the interferometric procedure. First, a relative phase θ is imprinted between the wells. Then, the BECs are released from the trap and form an interference pattern. The detectors (symbolically represented as open squares) measure the positions of atoms and these data are a starting point for the phase estimation.

In the remainder of this section, we will derive a compact and useful expression for $p_N(\vec{x}_N|\theta)$. Firstly, we decompose the initial state in the well-population basis, $|\psi_{\rm in}\rangle = \sum_{n=0}^{N} C_n|n, N-n\rangle$, and suppose that the expansion coefficients are real and possess the symmetry $C_n = C_{N-n}$. As we will argue later, such a choice of C_ns is natural in the context of this work. We switch from the Schrödinger to the Heisenberg representation, where the field operator evolves according to

$$\hat{\Psi}_\theta(x,t) \equiv \hat{U}^\dagger(\theta)\hat{\Psi}(x,t)\hat{U}(\theta) = \psi_a(x,t)\mathrm{e}^{\mathrm{i}\theta/2}\hat{a} + \psi_b(x,t)\mathrm{e}^{-\mathrm{i}\theta/2}\hat{b}.$$

The next step is to introduce the basis of the coherent phase states [29] defined as

$$|\varphi, N\rangle = \frac{1}{\sqrt{2^N N!}}\left(\hat{a}^\dagger + \mathrm{e}^{\mathrm{i}\varphi}\hat{b}^\dagger\right)^N |0\rangle$$

(where $|0\rangle$ is the state with zero particles). The action of the field operator on these states can be written in a simple form,

$$\hat{\Psi}_\theta(x,t)|\varphi, N\rangle = \sqrt{\frac{N}{2}}u_\theta(x,\varphi;t)|\varphi, N-1\rangle,$$

where $u_\theta(x,\varphi;t) = \psi_a(x,t)\mathrm{e}^{(\mathrm{i}/2)(\theta+\varphi)} + \psi_b(x,t)\mathrm{e}^{-(\mathrm{i}/2)(\theta+\varphi)}$. Next, we expand the Fock states in the basis of the coherent states,

$$|n, N-n\rangle = \sqrt{2^N}\frac{1}{\sqrt{\binom{N}{n}}}\int_0^{2\pi}\frac{\mathrm{d}\varphi}{2\pi}\mathrm{e}^{-\mathrm{i}\varphi(N-n)}|\varphi, N\rangle.$$

Thus, we can easily write the result of the action of the field operator on the input state,

$$\hat{\Psi}_\theta(x,t)|\psi_{\rm in}\rangle = \sqrt{\frac{2^N N}{2}} \sum_{n=0}^{N} \frac{C_n}{\sqrt{\binom{N}{n}}} \int_0^{2\pi} \frac{{\rm d}\varphi}{2\pi} {\rm e}^{-{\rm i}\varphi(N-n)} u_\theta(x,\varphi;t)|\varphi, N-1\rangle. \tag{2}$$

Now the calculation of $G_N(\vec{x}_N,\theta)$, and in turn of $p_N(\vec{x}_N,\theta)$, is straightforward and gives

$$p_N(\vec{x}_N|\theta) = \int_0^{2\pi}\int_0^{2\pi} \frac{{\rm d}\varphi}{2\pi}\frac{{\rm d}\varphi'}{2\pi} \prod_{i=1}^{N} u_\theta^*(x_i,\varphi;t)u_\theta(x_i,\varphi';t) \times \sum_{n,r=0}^{N} \frac{C_n C_r \cos\left[\varphi\left((N/2)-n\right)\right]\cos\left[\varphi'\left((N/2)-r\right)\right]}{\sqrt{\binom{N}{n}\binom{N}{r}}}. \tag{3}$$

In the following, we will consider an expansion time t large enough so that the interference pattern is well formed. In this regime, which is typically reached in experiments, the physical properties of the system change only by scaling $\sim\sqrt{t}$ of the characteristic dimensions of the cloud. The probability (3) is the starting point for the following discussion of various phase estimation strategies.

3. Estimation via the position of all *N* atoms

The first estimation protocol that we consider is based on the measurement of the position of all N atoms, described by the probability (3). This means that, in each realization of the experiment, the vector of positions $\vec{x}_N = (x_1 \cdots x_N)$ is obtained. According to the Cramér–Rao theorem [30, 31], the lower bound for the error on the phase inferred using $\vec{x}_N = (x_1 \cdots x_N)$ is given by

$$\Delta^2\theta = \frac{1}{F}, \tag{4}$$

where F is the Fisher information (FI),

$$F = m\int {\rm d}\vec{x}_N \frac{1}{p_N(\vec{x}_N|\theta)}\left(\frac{\partial p_N(\vec{x}_N|\theta)}{\partial\theta}\right)^2. \tag{5}$$

Here, m is the number of independent measurements used to infer the value of the phase θ. Any estimator $\theta_{\rm est}(\vec{x}_N)$, depending on $p_N(\vec{x}_N|\theta)$ only, will have an error equal to or larger than (4).

Among those estimators, the maximum-likelihood estimator (MLE) is an optimal choice, since, according to Fisher's theorem [30, 31], it saturates the Cramér–Rao lower bound (CRLB) (4). The MLE consists in inferring the value of the phase by maximizing, given the measurement outcomes $\vec{x}_N$, the probability $p_N(\vec{x}_N|\theta)$. More precisely, if m independent sets of measurements $\vec{x}_N^{(i)}$, $i = 1,\ldots,m$ are used to infer a single value of the phase, the MLE is given by $\theta_{\rm MLE}(\vec{x}_N^{(1)},\ldots,\vec{x}_N^{(m)})$ such that

$$\frac{\partial}{\partial\theta}\prod_{i=1}^{m} p_N(\vec{x}_N^{(i)}|\theta)\bigg|_{\theta=\theta_{\rm MLE}} = 0. \tag{6}$$

For a number of measurements m much larger than one, the phase estimation error, set by the variance of the $\theta_{\rm MLE}$, will be given by (4).

Now, in order to evaluate the phase estimation error, we need to calculate the FI (5). This can be done analytically, with the realistic assumption, discussed above, that the interference

pattern is formed after a sufficiently long expansion time, such that the wave-packet function can be explicitly written as

$$\psi_{a/b}(x,t) \simeq \mathrm{e}^{\mathrm{i}\frac{x^2}{2\tilde{\sigma}^2} \mp \mathrm{i}\frac{x\cdot x_0}{\tilde{\sigma}^2}} \cdot \tilde{\psi}\left(\frac{x}{\tilde{\sigma}^2}\right), \tag{7}$$

where $\tilde{\sigma} = \sqrt{\frac{\hbar t}{M}}$, $\tilde{\psi}$ is a Fourier transform of the initial wave packets, common to ψ_a and ψ_b, the separation of the wells is $2x_0$, and the particle mass is M. Moreover, we make a further realistic assumption that the initial separation of the wells of the trapping potential is much larger than the width of the mode functions.

We insert expression (7) into equation (3) and note that the N-body probability can be written as

$$p_N(\vec{x}_N|\theta) = [f(\vec{x}_N|\theta)]^2, \tag{8}$$

where f is real and reads

$$f(\vec{x}_N|\theta) = 2^N \int_0^{2\pi} \frac{\mathrm{d}\varphi}{2\pi} \sum_{n=0}^{N} \frac{C_n \cos\left[\varphi\left((N/2)-n\right)\right]}{\sqrt{\binom{N}{n}}} \prod_{i=1}^{N} \tilde{\psi}\left(\frac{x_i}{\tilde{\sigma}^2}\right) \cos\left(\frac{x_0 x_i}{\tilde{\sigma}^2} + \frac{\theta}{2} + \frac{\varphi}{2}\right). \tag{9}$$

This probability is put into the definition of the FI (5) to obtain

$$F = m \cdot 4 \int \mathrm{d}\vec{x}_N [f(\vec{x}_N|\theta)]^2.$$

Now the order of integration can be reversed and the space integrals performed first. Since the mode-functions are normalized, the result is

$$F = mN2^N \sum_{n=0}^{N} \frac{C_n^2}{\binom{N}{n}} \int_0^{2\pi} \frac{\mathrm{d}\varphi}{2\pi} \cos\left[\varphi(N-2n)\right] \left[N\left(\cos(\varphi)\right)^N - (N-1)\left(\cos(\varphi)\right)^{N-2}\right].$$

The phase integral can now be easily evaluated, giving

$$F = m \cdot 4 \sum_{n=0}^{N} C_n^2 \left(n - \frac{N}{2}\right)^2 = m \cdot 4\Delta^2 \hat{J}_z = F_Q. \tag{10}$$

Here, F_Q denotes the QFI, which is the maximal value of the FI with respect to all possible measurements [25], and depends therefore only on the interferometric transformation (in our case the phase shift) and the input state. For pure input states, the value of QFI is given by $4m$ times the variance of the phase-shift generator, and reads $F_\mathrm{Q} = m \cdot 4\Delta^2 \hat{J}_z$. Therefore, equation (10) contains a very remarkable result: the measurement of the position of all N atoms in the cloud is optimal, i.e. the best possible choice of the estimation strategy.

At this point, it is important to know whether the above optimal measurement can also reach sub-shot-noise sensitivities and for which input states this does happen. In order to investigate the possible values of the FI (10), we introduce a family of input states $\mathcal{A}$, defined using the two-mode Hamiltonian

$$\hat{H} = -E_J \hat{J}_x + \frac{E_\mathrm{C}}{N} \hat{J}_z^2. \tag{11}$$

We construct $\mathcal{A}$ by finding ground states of the above Hamiltonian for various values of the ratio $\gamma = \frac{E_\mathrm{C}}{NE_J}$. And so, for $\gamma > 0$, the elements of $\mathcal{A}$ are number-squeezed states and

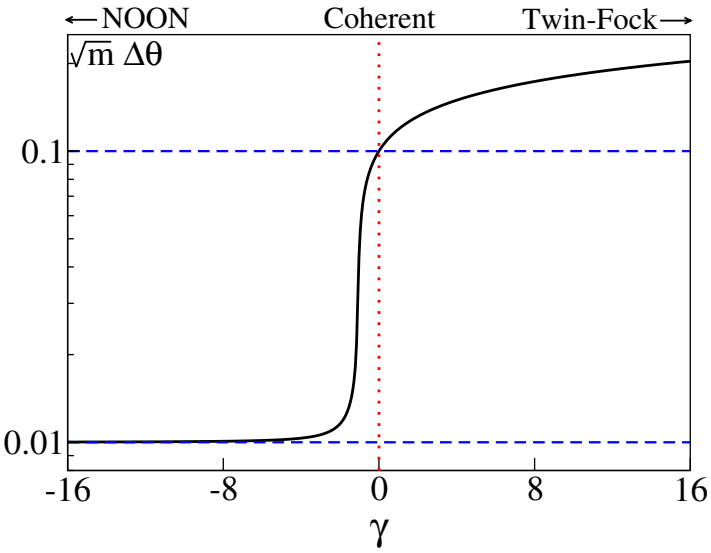

Figure 2. The sensitivity $\sqrt{m}\Delta\theta$ calculated with equation (10) (black solid line) for $N = 100$ atoms as a function of $|\psi_{\rm in}\rangle \in \mathcal{A}$ with $\gamma < 0$. The two limits, $\sqrt{m}\Delta\theta_{\rm SN}$ and $\sqrt{m}\Delta\theta_{\rm HL}$, are denoted by the upper and lower dashed blue lines, respectively. The sub-shot-noise sensitivity is obtained for all of the phase-squeezed states, $|\psi_{\rm in}\rangle \in \mathcal{A}$ with $\gamma < 0$. The vertical red dotted line denotes the position of the coherent state.

tend to the twin-Fock state $|\psi_{\rm in}\rangle = |\frac{N}{2}, \frac{N}{2}\rangle$ with $\gamma \to \infty$. For $\gamma < 0$, the elements of $\mathcal{A}$ are phase-squeezed states [23]. With $\gamma \to -\infty$, the ground state of (11) tends to the NOON state $|\psi_{\rm in}\rangle = \frac{1}{\sqrt{2}}(|N0\rangle + |0N\rangle)$. With $\gamma = 0$, we have a coherent state, $|\psi_{\rm in}\rangle = \frac{1}{\sqrt{N!}}\left(\frac{\hat{a}^\dagger + \hat{b}^\dagger}{\sqrt{2}}\right)^N |0\rangle$. Note that for all $|\psi_{\rm in}\rangle \in \mathcal{A}$, the coefficients C_n, which were introduced in the previous section, are real and symmetric. The choice of the ensemble $\mathcal{A}$ provides the different kinds of entangled states that are generally relevant for sub-shot-noise interferometry. The study of realistic protocols for the preparation of such states and the dynamical implementation of the phase shifter is beyond the scope of this work [23]. Our approximation, by which the phase shift transformation (1) acts simply on the ground state, would be realistic only when, after the ground state is prepared, the two clouds are split over a time scale much faster than the hopping rate set by E_J, but not fast enough to excite other modes. We also assume, as stated above, that the atom–atom interactions are negligible over the phase shift time scale. To this end, one can employ Feschbach resonances in order to tune the value of the scattering length very close to zero. The impact of residual interactions on the sensitivity of a double-well interferometer is beyond the scope of this work. For instance, in an MZI, it has been shown [24] that the residual inter-atomic interactions do not sensibly spoil the sensitivity.

It is straightforward to demonstrate that the value of FI in equation (10) gives the shot noise (SN) scaling, $\Delta\theta = \Delta\theta_{\rm SN} = \frac{1}{\sqrt{mN}}$ for the coherent state ($\gamma = 0$), and overcomes this bound for all $|\psi_{\rm in}\rangle \in \mathcal{A}$ with $\gamma < 0$, i.e. for the phase-squeezed states. The NOON state gives the Heisenberg limit, $\Delta\theta = \Delta\theta_{\rm HL} = \frac{1}{\sqrt{m}}\frac{1}{N}$. In figure 2, we plot the sensitivity calculated with equation (10) as a function of $|\psi_{\rm in}\rangle \in \mathcal{A}$ for $N = 100$ atoms.

We have thus shown that the measurement of the position of all of the atoms in the cloud is not only optimal but also reaches sub-shot-noise sensitivities for the phase-squeezed input state and saturates even the Heisenberg limit for the NOON state. The experimental feasibility of such a phase estimation strategy deserves some discussion. In the context of BEC, the typical number of atoms in the condensate implies that the above correlation function involves a very large configurational space of $\vec{x}_N$, which would be very hard to probe experimentally. Indeed, before the phase estimation can be performed, the probability $p_N(\vec{x}_N|\theta)$ (to be maximized according to MLE) must be experimentally reconstructed for different, and known, values of θ. The latter calibration stage would therefore involve a very large number of iterations.

This problem can be avoided in the context of optics, where entangled states of only a few photons have already been created experimentally [32–35]. The implementations with a very few particles, even though of small technological relevance (the quantitative difference between the shot-noise limit and the Heisenberg limit is small), would be important proof-of-principle experiments. Another necessary experimental tool is single-particle detection, which is of sufficiently high efficiency. In the context of BEC, very relevant experimental developments in this direction have been demonstrated in [36].

In the following section, we present a phase estimation scheme based on the measurement of the center of mass of the interference pattern. Although the probability of measuring the center of mass at position x is a function of just a one-dimensional (1D) variable, contrary to the N-dimensional vector $\vec{x}_N$, it can still provide the sub-shot-noise sensitivity. Nevertheless, we will demonstrate that sub-shot-noise interferometry with this estimation protocol is still challenging in the context of BEC.

4. Estimation via the center-of-mass measurement

4.1. Measurement of all N atoms

In the phase estimation protocol based on the position of the center of mass, the variable involved is the average $\frac{1}{N}\sum_{i=1}^{N} x_i$, resulting from the measurement of $\vec{x}_N$. The probability $p_{\rm cm}(x|\theta)$ describing this measurement is thus a function of a 1D variable, which implies a much less demanding calibration stage with respect to $p_N(\vec{x}_N|\theta)$.

The expression for this function can be extracted from the full N-body probability (3) by

$$p_{cm}(x|\theta) = \int \mathrm{d}\vec{x}_N\, \delta\left(x - \frac{1}{N}\sum_{i=1}^{N} x_i\right) p_N(\vec{x}_N|\theta),$$

where 'δ' is the Dirac delta. In order to provide an analytical expression, we model this time the mode-functions by Gaussians

$$\tilde{\psi}\left(\frac{x}{\tilde{\sigma}^2}\right) = \left(\frac{2\sigma_0^2}{\pi\tilde{\sigma}^4}\right)^{(1/4)} \mathrm{e}^{-x^2\sigma_0^2/\tilde{\sigma}^4} \tag{12}$$

with the initial width $\sigma_0 = 0.1$ and half of the well separation $x_0 = 1$. Using again the assumption that the initial separation of the wave packets is much larger than their width, i.e. $\mathrm{e}^{-{x_0}^2/{\sigma_0}^2} \ll 1$, we obtain

$$p_{cm}(x|\theta) = \sqrt{\frac{2\sigma_0^2 N}{\pi\tilde{\sigma}^4}}\mathrm{e}^{-2x^2\sigma_0^2/\tilde{\sigma}^4 N}\left[1 + \frac{1}{2}(C_0 + C_N)^2\cos\left(N\theta + \frac{2Nx_0}{\tilde{\sigma}^2}x\right)\right]. \tag{13}$$

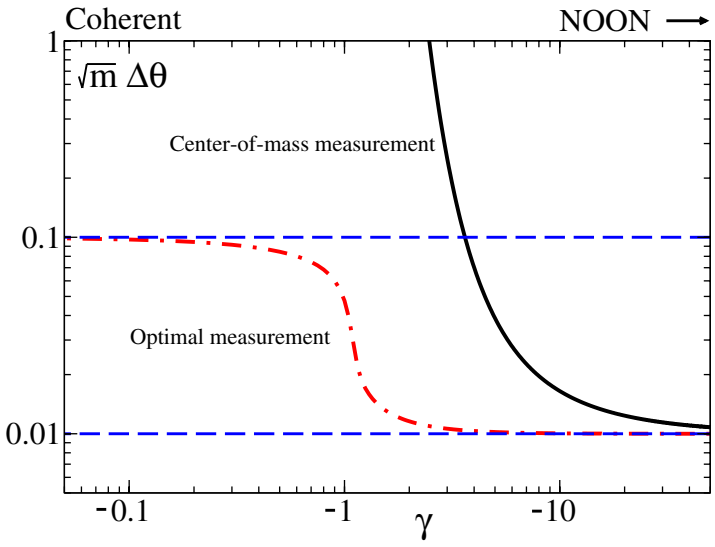

Figure 3. The sensitivity $\sqrt{m}\Delta\theta$ (black solid line) for $N = 100$ atoms calculated with equation (14) as a function of $|\psi_{\rm in}\rangle \in \mathcal{A}$ with $\gamma < 0$. The values of $\sqrt{m}\Delta\theta_{\rm SN}$ and $\sqrt{m}\Delta\theta_{\rm HL}$ are denoted by the upper and lower dashed blue lines, respectively. The optimal sensitivity, given by the inverse of the QFI, is drawn with the red open circles.

Details of this derivation are presented in appendix A. It is important to note that $p_{\rm cm}(x|\theta)$ depends on θ only for states with nonnegligible NOON components C_0 and C_N, as already noted in [37].

Once $p_{\rm cm}(x|\theta)$ is known, the phase can be estimated using the MLE, as described in the previous section. In this case, once again, the sensitivity is given by the inverse of the CRLB (4), where this time the FI is given by

$$F_{\rm cm} = m\int_{-\infty}^{\infty}\frac{{\rm d}x}{p_{\rm cm}(x|\theta)}\left(\frac{\partial}{\partial\theta}p_{\rm cm}(x|\theta)\right)^2$$
$$= mN^2\left[1-\sqrt{1-\frac{1}{2}(C_0+C_N)^2}\right], \qquad (14)$$

where m is the number of independent experiments used to infer the value of θ. In figure 3, we plot the sensitivity calculated by the inverse of the FI (14) as a function of $|\psi_{\rm in}\rangle \in \mathcal{A}$ with $\gamma \leqslant 0$. Although the estimation through the center of mass is not optimal ($\Delta\theta > \frac{1}{\sqrt{F_{\rm Q}}}$), the sensitivity can be better than the shot noise, with $\Delta\theta \to \Delta\theta_{\rm HL}$ for $|\psi_{\rm in}\rangle \to$ NOON.

As discussed above, an advantage of the center-of-mass estimation protocol is that the calibration stage is not as difficult as in the case of the Nth-order correlation function. However, in order to reach a sub-shot-noise phase sensitivity, it is necessary to detect all N atoms [38–41], as we show below.

4.2. Measurement of $k < N$ atoms

If the measurement of the center of mass is based on the detection of $k < N$ atoms, the probability (13) becomes

$$p_{cm}^{(k)}(x|\theta) = \int \mathrm{d}\vec{x}_k \, \delta\left(x - \frac{1}{k}\sum_{i=1}^{k} x_i\right) p_k(\vec{x}_k|\theta), \tag{15}$$

where $p_k(\vec{x}_k|\theta) = \int \mathrm{d}\vec{x}_{N-k} p_N(\vec{x}_N|\theta)$. The probability (15) can be calculated in a manner similar to that presented in appendix A. The result is

$$p_{cm}^{(k)}(x|\theta) = \sqrt{\frac{2\sigma_0^2 k}{\pi\tilde{\sigma}^4}} \mathrm{e}^{-(2x^2\sigma_0^2/\tilde{\sigma}^4)k} \left[1 + a\cos\left(k\theta + \frac{2kx_0}{\tilde{\sigma}^2}x\right)\right], \tag{16}$$

where

$$a = 2\sum_{i=0}^{N-k} \binom{(N-k)}{i} \frac{C_i C_{i+k}}{\sqrt{\binom{N}{i+k}\binom{N}{i}}}. \tag{17}$$

Note that for $k = N$, we recover the result from the previous section $a = 2C_0C_N = \frac{1}{2}(C_0 + C_N)^2$ (we are using the symmetric states, $C_0 = C_N$). The FI for the probability (16) can be calculated analytically,

$$F = mk^2(1 - \sqrt{1 - a^2}). \tag{18}$$

Let us now evaluate a and thus F for various $k \simeq N$. For $k = N$ and the NOON state in input, we have $C_0 = C_N = \frac{1}{\sqrt{2}}$, giving $a = 1$ and $F = mN^2$. From equation (17), we note that, for any k, a is the sum of $N - k$ terms, each depending on the coefficients C_i and C_{i+k}. And so, for $k = N - 1$, a will be maximal for a NOON-like state with $C_0 = C_{N-1} = \frac{1}{2}$ and $C_1 = C_N = \frac{1}{2}$. For this state, we obtain $a = \frac{1}{\sqrt{N}}$, and for large N, the value of the FI is $F = mN$.

Therefore, phase estimation using the center of mass of $N - 1$ particles gives a sensitivity bounded by the shot noise. Each loss of an atom decreases the FI roughly by a factor of N, drastically deteriorating the sensitivity. In figure 4, we plot the sensitivity $\sqrt{m}\Delta\theta$ calculated with the FI from equation (18) for various $k \simeq N$. To calculate a, we choose a subset of $|\psi_{\mathrm{in}}\rangle \in \mathcal{A}$ that is in the vicinity of the NOON state. The figure shows a dramatic loss of sensitivity as soon as $k \neq N$.

5. Estimation via the position measurement with the Mach–Zehnder interferometer (MZI)

5.1. Formulation

So far, we have focused on the position measurement of atoms released from a double-well trap, and studied the phase estimation sensitivity. We have seen that both the measurement of the position of all of the atoms in the cloud and the measurement of their center of mass allow for sub-shot-noise phase estimation. We have also seen that it would be challenging to beat the shot-noise limit using the above estimation strategies, at least when a large number of particles are involved.

In the above scenario, the sub-shot-noise sensitivity, which relies on nonclassical *particle* correlations, is reached by directly measuring spatial correlations between the atoms forming

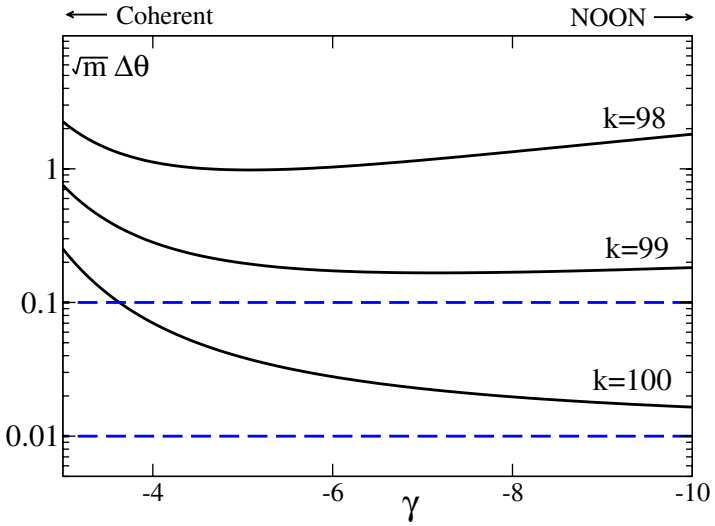

Figure 4. The sensitivity $\sqrt{m}\Delta\theta$ (black solid line) for $N = 100$ calculated with equation (18) as a function of $|\psi_{\text{in}}\rangle \in \mathcal{A}$ with $\gamma < 0$. The values of $\sqrt{m}\Delta\theta_{\text{SN}}$ and $\sqrt{m}\Delta\theta_{\text{HL}}$ are denoted by, respectively, the upper and lower dashed blue lines. The three solid lines correspond to the phase sensitivity for the estimation of the center of mass with different numbers of particles. For $k = 100$, the sensitivity is below the shot noise and tends to $\sqrt{m}\Delta\theta_{\text{HL}}$ for $|\psi_{\text{in}}\rangle \to$ NOON. As soon as $k \neq N$, the sub-shot-noise sensitivity is lost and the value of $\sqrt{m}\Delta\theta$ increases dramatically.

the interference pattern, and subsequently using the latter as estimators for the phase shift. On the other hand, it is well known that the MZI can easily provide sub-shot-noise sensitivity just by a simple measurement of the population imbalance between the two arms and a proper choice of the input state $|\psi_{\text{in}}\rangle$ [42]. The high sensitivity achievable with this interferometer has also been demonstrated in a realistic implementation with a BEC inside a double well [24]. This is because, in the MZI, the correlations between the two modes carry the part of the information contained in the particle correlations that is useful for phase estimation. When the clouds are released from the trap and the two modes start to overlap, the correlations between the two modes are lost, since an atom detected in the overlap region cannot be said to have come from either of the two initially separated clouds. This is the reason why it is necessary then to use directly high-order spatial correlations in order to reach sub-shot-noise sensitivity.

It would thus be interesting to quantify the effect of the overlap of the wave packets on the sensitivity of the MZI. This analysis is also of practical interest since, in the implementation of the atomic MZI, the precision of the population imbalance measurement can be improved by opening the trap and letting the clouds expand for a while. In this way, the density of the clouds drops, facilitating the measurement of the number of particles. However, during the expansion, the clouds inevitably start to overlap, leading to loss of information about the origin of the particles, as noted above. In this section, we show how the increasing overlap deteriorates the sensitivity of the MZI in two different estimation scenarios.

The MZI consists of three stages: two beam splitters represented by unitary evolution operators $e^{\mp i(\pi/2)\hat{J}_x}$ separated by the phase shifter $e^{-i\theta\hat{J}_z}$. The atomic MZI can be realized as

follows. Consider a two-mode system governed by the Hamiltonian (11) with $E_C = 0$. The first beam splitter is implemented by letting the atoms tunnel between the two wells for $t = \frac{\pi}{2}\frac{\hbar}{E_J}$, so the unitary evolution operator reads $\hat{U}_1 = \mathrm{e}^{-\mathrm{i}(\pi/2)\hat{J}_x}$. Then, the inter-well barrier is raised in order to suppress the hopping ($E_J = 0$), thereby implementing the phase shift transformation $\hat{U}_2 = \mathrm{e}^{-\mathrm{i}\theta\hat{J}_z}$. The interferometric sequence is closed by another beam splitter, $\hat{U}_3 = \mathrm{e}^{\mathrm{i}(\pi/2)\hat{J}_x}$. The full evolution operator reads

$$\hat{U}(\theta) = \hat{U}_3\hat{U}_2\hat{U}_1 = \mathrm{e}^{\mathrm{i}(\pi/2)\hat{J}_x}\mathrm{e}^{-\mathrm{i}\theta\hat{J}_z}\mathrm{e}^{-\mathrm{i}(\pi/2)\hat{J}_x} = \mathrm{e}^{-\mathrm{i}\theta\hat{J}_y},$$

where we used the commutation relations of the angular momentum operators.

In order to analyze the sensitivity of the MZI, we need to calculate the conditional probability $p_N(\vec{x}_N|\theta)$ of detecting N atoms at positions $\vec{x}_N = x_1 \cdots x_N$, as done in section 2 for the other interferometer discussed above. To evaluate this probability for any initial state of the double-well system $|\psi_{\mathrm{in}}\rangle$, we take the same steps as those taken to obtain equation (3). In the Heisenberg representation, the field operator evolves, under the MZI transformation, as

$$\hat{\Psi}_\theta(x,t) \equiv \hat{U}^\dagger(\theta)\hat{\Psi}(x,t)\hat{U}(\theta) = \left[\psi_a(x,t)\cos\left(\frac{\theta}{2}\right) + \psi_b(x,t)\sin\left(\frac{\theta}{2}\right)\right]\hat{a} + \left[\psi_b(x,t)\cos\left(\frac{\theta}{2}\right) - \psi_a(x,t)\sin\left(\frac{\theta}{2}\right)\right]\hat{b}. \tag{19}$$

Again, we express the action of the field operator on $|\psi_{\mathrm{in}}\rangle$ using the basis of the coherent phase states and obtain equation (2) with

$$u_\theta(x,\varphi;t) = \left[\psi_a(x,t)\cos\left(\frac{\theta}{2}\right) + \psi_b(x,t)\sin\left(\frac{\theta}{2}\right)\right]\mathrm{e}^{\mathrm{i}(\varphi/2)} + \left[\psi_b(x,t)\cos\left(\frac{\theta}{2}\right) - \psi_a(x,t)\sin\left(\frac{\theta}{2}\right)\right]\mathrm{e}^{-\mathrm{i}(\varphi/2)}.$$

Therefore, the probability $p_N(\vec{x}_N|\theta)$ for the MZI is given by equation (3) with the $u_\theta(x,\varphi;t)$ function defined above.

5.2. *Measurement of the population imbalance*

The most common phase-estimation protocol discussed in the context of the MZI is the measurement of the population imbalance between the two arms of the interferometer. In order to assess how the sensitivity of this protocol is influenced by the expansion of the wave packets, we introduce the probability of measuring n_L atoms in the left sub-space as follows,

$$p_{\mathrm{imb}}(n_{\mathrm{L}}|\theta) = \binom{N}{n_{\mathrm{L}}}\int_{-\infty}^{0}\mathrm{d}\vec{x}_{n_{\mathrm{L}}}\int_{0}^{\infty}\mathrm{d}\vec{x}_{N-n_{\mathrm{L}}}\, p_N(\vec{x}_N|\theta). \tag{20}$$

This probability depends on the expansion time via $\psi_{a,b}(x,t)$, which enter the definition of $p_N(\vec{x}_N|\theta)$. Note that the population imbalance probability can be written as

$$p_{\mathrm{imb}}(n_{\mathrm{L}}|\theta) = \int_0^{2\pi}\int_0^{2\pi}\frac{\mathrm{d}\varphi}{2\pi}\frac{\mathrm{d}\varphi'}{2\pi}\binom{N}{n_{\mathrm{L}}}a_\theta^{n_{\mathrm{L}}}b_\theta^{N-n_{\mathrm{L}}}\sum_{n,r=0}^{N}\frac{C_nC_r\cos[\varphi\,((N/2)-n)]\cos\left[\varphi'\,((N/2)-r)\right]}{\sqrt{\binom{N}{n}\binom{N}{r}}},$$

where

$$a_\theta = \int_{-\infty}^{0} \mathrm{d}x\, u_\theta^*(x,\varphi;t)u_\theta(x,\varphi';t) \quad \text{and} \quad b_\theta = \int_{0}^{\infty} \mathrm{d}x\, u_\theta^*(x,\varphi;t)u_\theta(x,\varphi';t).$$

Since the distribution of n_L inside the phase integrals is binomial, the moments can be easily calculated.

In this case, we cannot analytically calculate the FI, and therefore we turn to a simpler way of estimating the bound for the sensitivity. Namely, for various expansion times, if $m \gg 1$ measurements are carried out, the sensitivity can be calculated using the error propagation formula,

$$\Delta^2\theta = \frac{1}{m}\frac{\Delta^2 n}{\left|\partial\langle n\rangle/\partial\theta\right|^2}, \tag{21}$$

where

$$\langle n\rangle = \sum_{n_\mathrm{L}=0}^{N} p_\mathrm{imb}(n_\mathrm{L}|\theta)\left(n_\mathrm{L} - \frac{N}{2}\right)$$

is the average value of the population imbalance and

$$\Delta^2 n = \sum_{n_\mathrm{L}=0}^{N} p_\mathrm{imb}(n_\mathrm{L}|\theta)\left(n_\mathrm{L} - \frac{N}{2}\right)^2 - \langle n\rangle^2$$

are the associated fluctuations. The two lowest moments of the probability (20) read

$$\langle n\rangle = \int_0^\infty \mathrm{d}x\, G_1(x|\theta) - \frac{N}{2} \quad \text{and} \quad \Delta^2 n = \frac{N^2}{4} - \int_0^\infty\int_{-\infty}^0 \mathrm{d}\vec{x}_2\, G_2(\vec{x}_2|\theta) - \langle n\rangle^2.$$

The correlation functions for the MZI read $G_1(x|\theta) = \langle\hat{\Psi}_\theta^\dagger(x,t)\hat{\Psi}_\theta(x,t)\rangle$ and $G_2(\vec{x}_2|\theta) = \langle\hat{\Psi}_\theta^\dagger(x_1,t)\Psi_\theta^\dagger(x_2,t)\hat{\Psi}_\theta(x_2,t)\hat{\Psi}_\theta(x_1,t)\rangle$, with the field operator from equation (19), and the averages calculated with the input state. When the two wave packets do not overlap, i.e. $\psi_a(x,t)\psi_b^*(x,t) \simeq 0$ for all $x \in \mathbb{R}$, equation (21) simplifies to

$$\Delta^2\theta = \frac{1}{m}\frac{\Delta^2\hat{J}_x\sin^2\theta + \langle\hat{J}_z^2\rangle\cos^2\theta}{\langle\hat{J}_x\rangle^2\cos^2\theta}. \tag{22}$$

This is the well-known expression for the sensitivity of the population imbalance between separated arms. It gives $\Delta\theta \leqslant \Delta\theta_\mathrm{SN}$ for all $|\psi_\mathrm{in}\rangle \in \mathcal{A}$ with $\gamma \geqslant 0$.

We investigate the impact of the overlap on the sensitivity (21) by modeling the free expansion of the wave packets $\psi_{a/b}(x,\tau)$ by Gaussians,

$$\psi_{a/b}(x,\tau) = \frac{1}{(2\pi\sigma_0^2(1+\mathrm{i}\tau))^{1/4}}\mathrm{e}^{-(x\pm x_0)^2/4\sigma^2(1+\mathrm{i}\tau)},$$

and take, as done in section 4, $x_0 = 1$ and the initial width $\sigma_0 = 0.1$. In figure 5, we plot the sensitivity $\sqrt{m}\Delta\theta$ taking $\theta = 0$ and $N = 100$ for three different expansion times τ. The initial sensitivity deteriorates as soon as the wave packets start to overlap, and the sub-shot-noise sensitivity is lost for long expansion times. As discussed above, we attribute this decline to the loss of information about the correlations between the modes. Therefore, special attention has to be paid to avoid the overlap when letting the two trapped condensates spread. Although we expect that the expansion facilitates the atom number measurement, the conclusion of this section is that any overlap of the spatial modes has a strong negative impact on the sensitivity of the MZI.

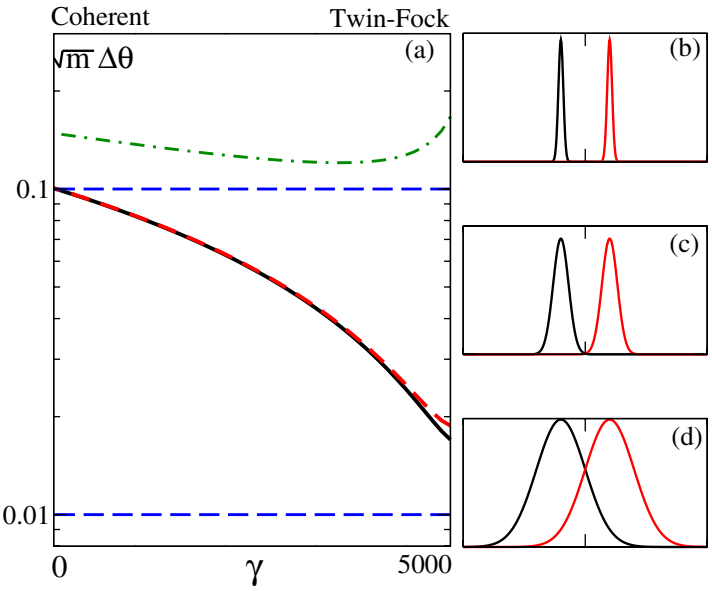

Figure 5. (a) The sensitivity $\sqrt{m}\Delta\theta$ calculated with equation (21) for three different expansion times τ as a function of $|\psi_{\rm in}\rangle \in \mathcal{A}$ with $\gamma \geqslant 0$. The solid black line corresponds to the situation shown in (b), where $\tau = 0$ and the wave packets do not overlap. The dashed red line corresponds to (c), where $\tau = 3$ and the wave packets start to overlap. The dot dashed green line corresponds to (d), where $\tau = 10$ and the wave packets strongly overlap. Clearly, the sensitivity is influenced by any nonvanishing overlap. The values of $\sqrt{m}\Delta\theta_{\rm SN}$ and $\sqrt{m}\Delta\theta_{\rm HL}$ are denoted by, respectively, the upper and lower dashed blue lines. Here, $N = 100$ and $\theta = 0$.

5.3. Estimation via the center-of-mass measurement for the MZI

In section 4.1, we demonstrated that when the two wave packets overlap and form an interference pattern, the phase estimation based on the center-of-mass measurement can give sub-shot-noise sensitivity. Here we study the same estimation strategy applied in the MZI case. Again, we start with the probability $p_{\rm cm}(x|\theta)$ of measuring the center of mass at position x,

$$p_{\rm cm}(x|\theta) = \int {\rm d}\vec{x}_N \, \delta\left(x - \frac{1}{N}\sum_{i=1}^{N} x_i\right) p_N(\vec{x}_N|\theta).$$

Using $p_N(\vec{x}_N|\theta)$ for the MZI, one can analytically calculate the center-of-mass probability only in the limit of small θ,

$$p_{\rm cm}(x|\theta) = \frac{N}{2\pi\sigma^2}\left[\sum_{l=0}^{N} C_l^2 f_l(x) + \theta \sum_{l=0}^{N} C_l C_{l+1}\sqrt{(l+1)(N-l)}\,(f_{l+2}(x) - f_l(x))\right], \tag{23}$$

where

$$f_l(x) = \exp\left[-\frac{(x - x_0\,((2l/N) - 1))^2}{2\sigma_0^2}\right].$$

With this probability, we can again calculate the sensitivity using the error propagation formula [30, 31],

$$\Delta^2\theta = \frac{1}{m}\frac{\Delta^2 x}{\left|\partial\langle x\rangle/\partial\theta\right|^2},$$

where

$$\langle x\rangle = \int_{-\infty}^{\infty} \mathrm{d}x\; p_{\mathrm{cm}}(x|\theta)x \quad \text{and} \quad \Delta^2 x = \int_{-\infty}^{\infty} \mathrm{d}x\; p_{\mathrm{cm}}(x|\theta)x^2 - \langle x\rangle^2.$$

These two moments can be easily calculated with equation (23), giving, in the limit $\theta \to 0$,

$$\Delta^2\theta\Big|_{\theta\to 0} = \frac{1}{m}\left[\frac{\langle \hat{J}_z^2\rangle}{\langle \hat{J}_x\rangle^2} + \left(\frac{\sigma}{x_0}\right)^2 \frac{N}{4\langle \hat{J}_x\rangle^2}\right]. \tag{24}$$

Note that when the initial size of the Gaussians tends to zero, we recover the sensitivity from equation (22) (in the limit of $\theta \to 0$). This is not surprising, because when the mode-functions are point-like, the measurement of the center of mass and the measurement of the population imbalance are equivalent, and related by $x_{\mathrm{cm}} = 2x_0\frac{n}{N}$. Therefore, for small σ, the measurement of the center of mass yields sub-shot-noise sensitivity for all $|\psi_{\mathrm{in}}\rangle \in \mathcal{A}$ with $\gamma > 0$. However, for nonzero σ, the second term in equation (24) spoils the sensitivity. This is because $\frac{N}{4\langle \hat{J}_x\rangle^2} \geqslant \frac{1}{N}$ is always satisfied. Even though the first term scales better than at the shot-noise limit, the other one does not, and will dominate for large N.

From what we presented in this section, we conclude that both the population imbalance and the center-of-mass measurements can give sub-shot-noise sensitivity for the MZI, but both are very sensitive to the growing size of the wave packets.

6. Conclusions

In this paper, we have discussed in detail how the measurement of the positions of atoms forming an interference pattern can be useful in the context of atom interferometry. We showed that phase estimation based on the measurement of the position of all the atoms in the cloud is an optimal detection strategy, saturating the QFI, and even reaching a Heisenberg-limited sensitivity when NOON states are used. We also showed that the measurement of the position of the center of mass of the interference pattern gives sub-shot-noise sensitivity for all states with a nonnegligible NOON component. The measurement of the positions of all atoms, and in turn of their center of mass, is difficult to carry out. The former requires the construction of a function of a highly dimensional configuration space, and both require the detection of all N atoms forming the interference pattern. We attribute the difficulty of obtaining the sub-shot-noise sensitivity to the fact that, after the formation of the interference pattern, the modes cannot be distinguished, and information useful for interferometry is only contained in the correlations between the particles. The implementation of any estimation strategy would also require an analysis of the impact of experimental noise on sensitivity, which is not included in this work. In the final part of this work, we turned our attention to the MZI, which is known to provide sub-shot-noise sensitivity for the simpler measurement of the population imbalance between the two clouds. We have shown that the sensitivity of the MZI is strongly influenced by a nonzero overlap between the two wave packets, in the case of both the population imbalance and the center-of-mass measurement.

Acknowledgments

This work was supported (JCh) by the Foundation for Polish Science through the TEAM project cofinanced by the EU European Regional Development Fund.

Appendix A. Evaluation of the center-of-mass probability

In this appendix, we derive the expression for the probability of detecting the center of mass at position x, as in equation (13). The definition of $p_{\rm cm}(x|\theta)$ relates it to the full N-body probability by

$$p_{\rm cm}(x|\theta) = \int \mathrm{d}\vec{x}_N\, \delta\left(x - \frac{1}{N}\sum_{i=1}^{N} x_i\right) p_N(\vec{x}_N|\theta).$$

To calculate this probability, we assume a long expansion time and use equations (8) and (9). Then, we note that the Dirac delta can be represented as the Fourier transform

$$p_{\rm cm}(x|\theta) = \frac{1}{2\pi}\int_{-\infty}^{\infty}\mathrm{d}k \int \mathrm{d}\vec{x}_N\, \mathrm{e}^{-\mathrm{i}k(x-(1/N))\sum_{i=1}^{N} x_i)}\, p_N(\vec{x}_N|\theta).$$

This equation can be rewritten as

$$p_{\rm cm}(x|\theta) = \frac{1}{2\pi}\int_{-\infty}^{\infty}\mathrm{d}k\, \mathrm{e}^{-\mathrm{i}kx}\, \tilde{p}_{\rm cm}(k|\theta), \tag{A.1}$$

where

$$\tilde{p}_{\rm cm}(k|\theta) = \int \mathrm{e}^{\mathrm{i}\frac{k}{N}\sum_{i=1}^{N} x_i}\, p_N(\vec{x}_N|\theta)\, \mathrm{d}\vec{x}_N$$

is the Fourier transform of the probability $\tilde{p}_{\rm cm}(x|\theta)$. To provide an analytical expression for this probability, we assume that the initial wave packets are Gaussian as in equation (12). Integration over space is performed, giving

$$\tilde{p}_{\rm cm}(k|\theta) = \int_0^{2\pi}\frac{\mathrm{d}\varphi}{2\pi}\int_0^{2\pi}\frac{\mathrm{d}\varphi'}{2\pi}\left[I(k,\varphi,\varphi')\right]^N \times \sum_{n,m=0}^{N}\frac{C_n C_m}{\sqrt{\binom{N}{n}\binom{N}{m}}}\cos\left[\varphi\left(\frac{N}{2}-n\right)\right]\cos\left[\varphi'\left(\frac{N}{2}-m\right)\right], \tag{A.2}$$

where

$$I(k,\varphi,\varphi') = \mathrm{e}^{\mathrm{i}\left(\frac{\varphi+\varphi'}{2}+\theta\right)}\mathrm{e}^{-\frac{(k+k_0)^2}{2w^2}} + \mathrm{e}^{-\mathrm{i}\left(\frac{\varphi+\varphi'}{2}+\theta\right)}\mathrm{e}^{-\frac{(k-k_0)^2}{2w^2}} + 2\cos\left(\frac{\varphi+\varphi'}{2}\right)\mathrm{e}^{-\frac{k^2}{2w^2}},$$

with $k_0 = \frac{2Nx_0}{\tilde{\sigma}^2}$ and $w = \frac{2N\sigma_0}{\tilde{\sigma}^2}$. The function $I(k,\varphi,\varphi')$ consists of three peaks, located at $k = \pm k_0$ and $k = 0$. When the well separation $2x_0$ is large compared to the initial width of the trapped wave packets σ, these three peaks are separated and do not overlap. Therefore, $[I(k,\varphi,\varphi')]^N$ can be approximated by the sum of the Nth powers of its three components,

$$\left[I(k,\varphi,\varphi')\right]^N \simeq \mathrm{e}^{\mathrm{i}N\left(\frac{\varphi+\varphi'}{2}+\theta\right)}\mathrm{e}^{-\frac{N(k+k_0)^2}{2w^2}} + \mathrm{e}^{-\mathrm{i}N\left(\frac{\varphi+\varphi'}{2}+\theta\right)}\mathrm{e}^{-\frac{N(k-k_0)^2}{2w^2}} + 2^N\cos^N\left(\frac{\varphi+\varphi'}{2}\right)\mathrm{e}^{-\frac{Nk^2}{2w^2}}.$$

This result is put into equation (A.2), the phase integrals are evaluated and the result is

$$\tilde{p}_{\mathrm{cm}}(k|\theta) = \mathrm{e}^{-N\frac{k^2}{2w^2}} + \left[\mathrm{e}^{\mathrm{i}N\theta - N\frac{(k+k_0)^2}{2w^2}} + \mathrm{e}^{-\mathrm{i}N\theta - N\frac{(k-k_0)^2}{2w^2}}\right]\frac{(C_0+C_N)^2}{4}.$$

Then, using equation (A.1), we obtain

$$p_{cm}(x|\theta) = \frac{w\,\mathrm{e}^{-(w^2x^2/2N)}}{\sqrt{2\pi N}}\left[1 + \frac{(C_0+C_N)^2}{2}\cos(N\theta + k_0 x)\right],$$

which, with the help of the definitions of w and k_0, gives equation(13).

References

[1] Mach E 2003 *The Principles of Physical Optics* (New York: Dover)
[2] Cronin A D, Schmiedmayer J and Pritchard D E 2009 *Rev. Mod. Phys.* **81** 1051
[3] Obrecht J M, Wild R J, Antezza M, Pitaevskii L P, Stringari S and Cornell E A 2007 *Phys. Rev. Lett.* **98** 063201
[4] Pasquini T A, Shin Y, Sanner C, Saba M, Schirotzek A, Pritchard D E and Ketterle W 2004 *Phys. Rev. Lett.* **93** 223201
[5] Lin Y J, Teper I, Chin C and Vuletić V 2004 *Phys. Rev. Lett.* **92** 050404
[6] Baumgärtner F, Sewell R J, Eriksson S, Llorente-García I, Dingjan J, Cotter J P and Hinds E A 2010 *Phys. Rev. Lett.* **105** 243003
[7] Fattori M, D'Errico C, Roati G, Zaccanti M, Jona-Lasinio M, Modugno M, Inguscio M and Modugno G 2008 *Phys. Rev. Lett.* **100** 080405
[8] Anderson B P and Kasevich M A 1998 *Science* **282** 1686
[9] Estève J, Gross C, Weller A, Giovanazzi S and Oberthaler M K 2008 *Nature* **455** 1216
[10] Gross C, Zibold T, Nicklas E, Estéve J and Oberthaler M K 2010 *Nature* **464** 1165
[11] Riedel M F, Bhi P, Li Y, Hnsch T W, Sinatra A and Treutlein P 2010 *Nature* **464** 1170
[12] Maussang K, Marti G E, Schneider T, Treutlein P, Li Y, Sinatra A, Long R, Estève J and Reichel J 2010 *Phys. Rev. Lett.* **105** 080403
[13] Giovanetti V, Lloyd S and Maccone L 2004 *Science* **306** 1330
[14] Pezzé L and Smerzi A 2009 *Phys. Rev. Lett.* **102** 100401
[15] Shin Y, Saba M, Pasquini T A, Ketterle W, Pritchard D E and Leanhardt A E 2004 *Phys. Rev. Lett.* **92** 050405
[16] Schumm T, Hofferberth S, Anderson L M, Wildermuth S, Groth S, Bar-Joseph I, Schmiedmayer J and Krüger P 2005 *Nat. Phys.* **1** 57
[17] Albiez M, Gati R, Fölling J, Hunsmann S, Cristiani M and Oberthaler M K 2005 *Phys. Rev. Lett.* **95** 010402
[18] Levy S, Lahoud E, Shomroni I and Steinhauer J 2007 *Nature* **449** 579
[19] LeBlanc L J, Bardon A B, McKeever J, Extavour M H T, Jervis D, Thywissen J H, Piazza F and Smerzi A 2011 *Phys. Rev. Lett.* **106** 025302
[20] Pezzé L, Collins L A, Smerzi A, Berman G P and Bishop A R 2005 *Phys. Rev.* A **72** 043612
[21] Lee C 2006 *Phys. Rev. Lett.* **97** 150402
[22] Huang Y P and Moore M G 2008 *Phys. Rev. Lett.* **100** 250406
[23] Grond J, Hohenester U, Mazets I and Schmiedmayer J 2010 *New J. Phys.* **12** 065036
[24] Grond J, Hohenester U, Schmiedmayer J and Smerzi A 2010 arXiv:1010.3273
[25] Braunstein S L and Caves C M 1994 *Phys. Rev. Lett.* **72** 3439
[26] Chwedeńczuk J, Piazza F and Smerzi A 2010 *Phys. Rev.* A **82** 051601
[27] Javanainen J and Yoo S M 1996 *Phys. Rev. Lett.* **76** 161
[28] Castin Y and Dalibard J 1997 *Phys. Rev.* A **55** 4330
[29] Mullin W J and Laloë F 2010 *Phys. Rev.* A **82** 013618
[30] Helstrom C W 1976 *Quantum Detection and Estimation Theory* (New York: Academic) chapter VIII

[31] Holevo A S 1982 *Probabilistic and Statistical Aspect of Quantum Theory* (Amsterdam: North-Holland)
[32] Walther P *et al* 2004 *Nature* **429** 158
[33] Ourjoumtsev A, Jeong H, Tualle-Brouri R and Grangier P 2007 *Nature* **448** 784
[34] Vahlbruch H *et al* 2008 *Phys. Rev. Lett.* **100** 033602
[35] Gao W B *et al* 2010 *Nat. Phys.* **6** 331
[36] Heine D *et al* 2010 *New J. Phys.* **12** 095005
[37] Bach R and Rzążewski K 2004 *Phys. Rev. Lett.* **92** 200401
[38] Dorner U, Demkowicz-Dobrzański R, Smith B J, Lundeen J S, Wasilewski W, Banaszek K and Walmsley I A 2009 *Phys. Rev. Lett.* **102** 040403
[39] Kacprowicz M, Demkowicz-Dobrzański R, Wasilewski W, Banaszek K and Walmsley I A 2010 *Nat. Photonics* **4** 357
[40] Kołodyński J and Demkowicz-Dobrzański R 2010 *Phys. Rev.* A **82** 053804
[41] Knysh S, Smelyanskiy V N and Durkin G A 2011 *Phys. Rev.* A **83** 021804(R)
[42] Pezzé L and Smerzi A 2006 *Phys. Rev.* A **73** 011801